Applied Physics A (2023) 129:445
https://doi.org/10.1007/s00339-023-06717-8

Applied Physics A
Materials Science & Processing

Electronic correlation effects in Ce_4RuMg compound

J. C. Debnath[1,2] · Shams Forruque Ahmed[1] · J. L. Wang[3,4]

Received: 27 March 2023 / Accepted: 9 May 2023 / Published online: 26 May 2023

Abstract
Different factors of electronic correlations directly relate with the fundamentals of condensed matter physics. Exploration of novel materials has an important character in developing the level of understanding of magnetic properties in correlated matters. It is known to all scientists that Cerium-based compounds exhibit different thought-provoking properties which relate with the correlated nature of intermetallics materials. To improve the knowledge of correlated systems especially at very low temperatures, we prepare a statement on Ce_4RuMg material. Different physical properties of the compound Ce_4RuMg have been measured within a range above room temperature to very low temperature which is about 0.5 K with the application of 7 T applied magnetics field. It is observed that the type of crystallization is cubic Gd_4RhIn type structure and the space group is F43m. An incongruity is perceived at 1.5 K from the magnetic susceptibility graph, a suggestion of the antiferromagnetic phase of that compound. The observed moment of magnetization is $\mu_{eff} = 2.17\ \mu_B$/Ce which is very close to pure Ce metal ($\mu_{eff} = 2.54\ \mu_B$). This might be associated with the (CEF) effects considering magnetocrystalline anisotropy. The zero magnetic field specific heat measurement exhibits an anomaly at 1.8 K which is possibly owing to the presence of long-range magnetic interactions in Ce_4RuMg. The value of electronic specific heat coefficient $\gamma = 137$ mJ/Ce-mol K^2, calculated from the heat capacity measurements, parades the tendency of a heavy fermion-like behavior.

Keywords Saturated moment · Effective magnetic moment · Antiferromagnetic · Heavy fermion

1 Introduction

Numerous aspects of electronic correlations always bring new pioneering and mysterious characteristics to the advancement of condensed matter physics. To enrich the knowledge of magnetism in the correlated matter, exploration of different materials and their structure always play an important key role. It is evident that Ce and Yb typed materials show sundry types of significant phenomena which are mostly heavy electron behaviors, mixed valence behavior, semiconductor and Kondo insulator, metal–insulator transition, and finally unusual superconductivity [1–12]. The appearance of these phenomena represents a solid hybridization between conduction and localized 4*f* electrons [1, 2, 4].

Magnetism and magnetic materials research fields always play a key role in the industry as well as in our daily life. That is why magnetic materials such as rare-earth based and intermetallics are always on the list of that research field. Rare-earth based materials are characterized by an incompletely filled 4*f* shell.

Magnetism in rare-earth-based compounds, mainly instigates from the partially filled 4*f* shell electrons and the magnetic moments are large for the well-localized electrons. These can also be characterized by considering low ordering temperature and strong single-ion magnetocrystalline anisotropy. Due to the interactions between localized 4*f* moments and the environment, unfamiliar low-temperature properties have been observed in a large group of rare-earth-based materials. Interesting magnetic properties have also been observed for the combination of

✉ J. C. Debnath
jyotish.debnath@auw.edu.bd; jcdebnath28@gmail.com

[1] Science and Math Program, Asian University for Women, Chattogram 4000, Bangladesh

[2] Highly Correlated Matter Research Group, Physics Department, University of Johannesburg, P.O. Box 524, Auckland Park 2006, South Africa

[3] Institute for Superconductivity and Electronic Materials, University of Wollongong, Wollongong, NSW 2522, Australia

[4] College of Physics, Jilin University, Changchun 130012, People's Republic of China

transition metals and rare-earths if the transition metals are weakly magnetic or even nonmagnetic.

Cerium intermetallics have been studied for many years relating to their unfamiliar magnetic properties. In these intermetallics, different electronic states can be espoused by cerium, which are paramagnetic or diamagnetic or intermediate valence, leading to heavy-fermion behavior, non-Fermi liquid behavior and magnetic ordering. The reason for these singularities is the hybridization between the conduction electrons and the 4*f*(Ce) [13–18].

It is vital to understand the magnetic and electronic behavior of Ce_4RuMg as intermetallic magnesium-based compounds plays substantial technical importance for slush hardening (microstructure and mechanical properties optimization) in the application of modern light weight alloys and hydrogen storage. Detailed crystal chemical structure and chemical bonding of Ce_4RuMg compound has been reported but fairly physical properties have been discussed [19, 20]. This crystallization of this compound occurs with the cubic Gd_4RhIn type structure and the space group is F43m. It is observed that cerium atoms form trigonal prisms with ruthenium at the center which are again topped by three additional cerium atoms on the rectangular faces [19, 21]. Over the years, a little study has been done on intermetallic magnesium-based systems with respect to magnetic properties. Especially low-temperature studies (< 2 K) are very rare for Ce_4RuMg material. In this paper, we represent a study on Ce_4RuMg at very low temperature to room temperature where at low temperature (< 2 K) a visible magnetic ordering has been observed for both susceptibility and heat capacity measurements, respectively.

2 Section for experimental

Synthesis of polycrystalline Ce_4RuMg was done from cerium ingots (refined 99.90%), ruthenium powder (refined 99.90%), and a rod of magnesium (refined 99.95%). First, the cerium ingots were arc-melted under cleansed argon. Then the cerium, ruthenium, and magnesium were measured in the proportion of 4:1:1. Then, arc-welded under the pressure of argon at about 800 mbar. Second, the vessel was inductively heated at about 1300 K for 2 min and finally for 2 h at the temperature of 920 K. Finally, the container was slaked to room temperature to separate the sample from the tube. X-ray diffraction shows that the crystallization of this compound occurs with the cubic Gd_4RhIn type structure and the space group is F43m, where $a = 1409.2$ (2) pm, $v = 2.7917$ nm^3 very close to the value of Tuncel et al. [21]. Measurements of physical properties were done using a standard PPMS (physical property measurement system).

3 Results and discussion

Figure 1 displays the representation of inverse magnetic susceptibility of Ce_4RuMg. The measurement has been taken with the temperature 0.4 K–400 K and a field of 0.05 T.

A fit of the inverse magnetic susceptibility is done using a modified Curie–Weiss expression $\chi^{-1}(T) = [\chi_0 + C/(T - \theta_P)]^{-1}$. The calculated effective magnetic moment is $\mu_{eff} = 2.17\ \mu_B$/Ce and the temperature-independent contribution $\chi_0 = 0.14715$ emu/Ce-mole.

This calculated value is lesser than the free ion Ce^{+3} value which is $\mu_{eff} = 2.54\ \mu_B$. The reason for the reduction of that value is that all cerium atoms are not in the trivalent state. Since it is mentioned before that trigonal prisms are formed by the atoms of cerium centering the ruthenium and again topped by three further cerium atoms on the rectangular faces [19, 21]. But this value is higher than that of Tappe et al. [19] which is 1.93 μ_B/Ce. The value of the Weiss constant of θ_P is − 20.5 K which is extrapolated from $\chi^{-1}(T)$ vs. T data. The minus sign of θ_P specifies the development of antiferromagnetic interactions in the paramagnetic region.

It is observed that the deviation of $\chi^{-1}(T)$ from Curie–Weiss behavior starts below 100 K. The reason behind that behavior is the crystal field splitting of the $J = 5/2$ ground state of Ce^{+3}. In addition, the commencement of magnetic interactions is short-ranged. The anomaly at low temperature (due to magnetic ordering) represents that the ordering is antiferromagnetic which is $T_N = 1.5$ K.

Magnetization vs magnetic field data (M-H) has been shown in Fig. 2. It is observed that a strong curvature in M (H) is evident for the curve at $T = 1.76$ K and a tendency to be saturated at higher fields, but the for the temperature 10 K, the graph tends to be almost linear from the low to high fields. For $T = 1.76$ K, the curvature is strong and

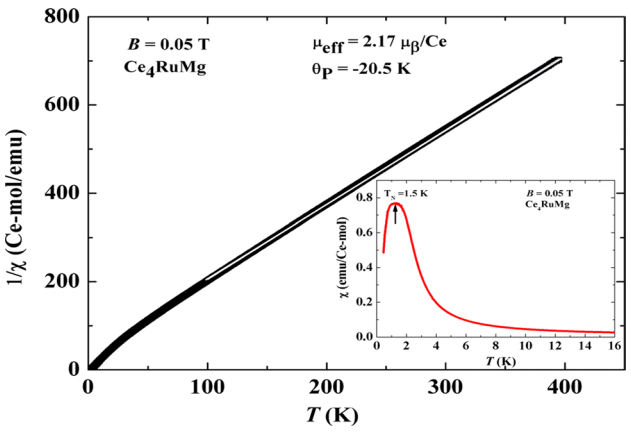

Fig. 1 $\chi^{-1}(T)$ vs T graph for the compound Ce_4RuMg with applied field 0.05 T. Inset: $\chi^{-1}(T)$ vs T graph at low temperatures, arrow indicates the irregularity due to magnetic ordering

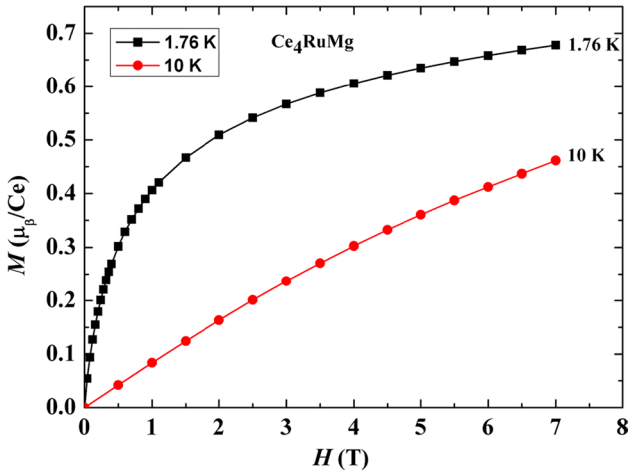

Fig. 2 The magnetization graph for the compound Ce_4RuMg at different temperatures and fields

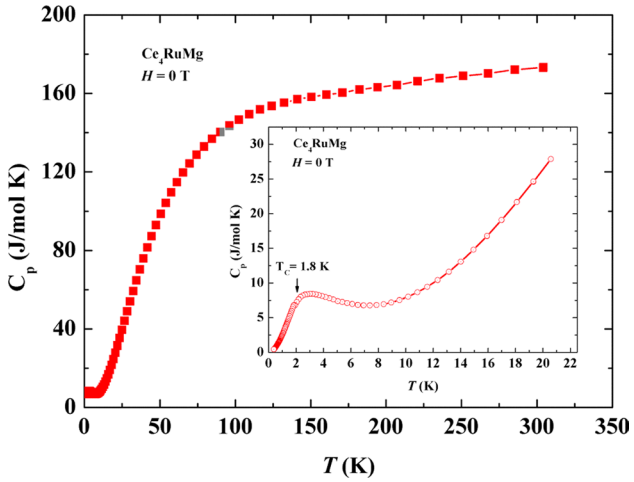

Fig. 3 Heat capacity graph for the temperature up to 300 K with zero applied field. Inset: C_P vs T graph for low-temperature region

dependent on the field in below 2 T region. The calculated moment at 1.76 K, with an applied field of 7 T is 0.68 μ_B / Ce, is very low compared to the theoretical value of saturated moment of free Ce^{+3} ion which is $\mu_s = 2.14\ \mu_B$. The magnetic moment observed by Tappe et al. [19] is 0.84 μ_B/ Ce for the temperature and applied field of 3 K and 8 T, respectively. It is predicted that this reduction is owing to the crystal field splitting of $J = 5/2$ and all the Ce atoms are not in the stable trivalent state.

The table shows a comparative study of Magnetic property for different materials (Table 1).

The heat capacity $C_P(T)$ graph of Ce_4RuMg with zero applied field is shown in the Fig. 3. An upturn is visible at 1.8 K, indicates the magnetic phase transition of that material which is shown in inset of the Fig. 3. This appeared phase transition (at 1.8 K) is compatible with the susceptibility measurement where a noticeable maximum is existing at 1.5 K (shown inset of Fig. 1).

The following equation represents the total heat capacity C_p of a compounds measurement system:

$$C_p = C_{el} + C_{ph} + C_{mag} \quad (1)$$

The right-hand terms C_{el}, C_{ph} and C_{mag} represent the electronic contribution, lattice contribution which is caused by the lattice vibrations and the magnetic contribution of $C_p(T)$ respectively. Again, we know that $C_{el} = \gamma T$, where γ is known as the electronic coefficient of specific heat. To calculate γ value we use the C_p/T *vs.* T^2 curve shown in Fig. 4. The observed upturn at low temperatures in the graph relates with the phase transition in a low magnetic field. We have calculated the value of γ which is 137 mJ/Ce-mol•K^2 for Ce_4RuMg, suggesting the presence of strong electronic correlations in Ce_4RuMg. The enhanced value of γ may be due to the short-range correlations immediately above T_N. The calculated value of θ_D is 180 K which is obtained from the simplified Debye model.

The following table illustrates a relative study of γ for different compounds (Table 2) [22–25].

Again, we have measured the heat capacity of Ce_4RuMg for low temperature (up to 26 K) at 0 T, 3 T and 5 T fields to analyze the state of specific heat of Ce_4RuMg, which is exposed in Fig. 5. At higher temperatures the peak shifts and becomes broader with increasing applied field, is the indication of second-order magnetic phase transition.

The following equation has been used to calculate the heat capacity with the addition of electronic contribution by the standard Debye formula:

Table 1 A comparative study of magnetic properties among different materials

Compound	μ_{eff}/ μ_B/Ce	θ_p/K	$\chi^{-1}(T)$/emu/mole^{-1}	μ_{sm}/ μ_B/Ce	References
Ce_4RuMg	2.17	− 20.5	0.14715	0.68	Present work
Ce_4RuMg	1.93	− 4.0	0.00252	0.84	[19]
Ce_4RuAl	1.73	− 34.1	0.0035	0.36	[19]
Ce4RuAl	2.18	− 81.33	0.0003668	0.25	[22]
CeRuAl	1.79	− 32.6	0.00042	0.60	[10]

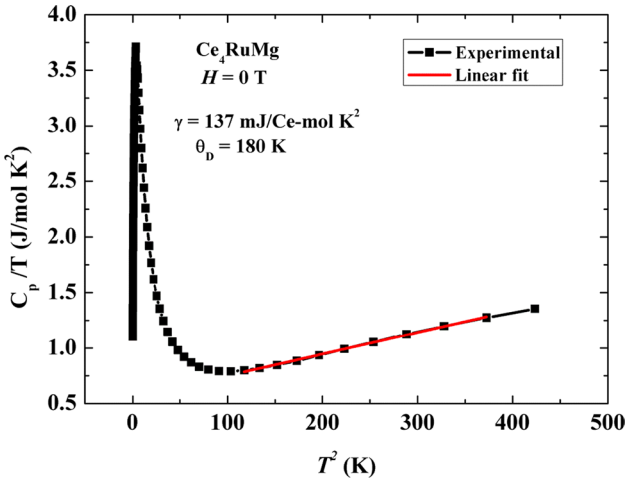

Fig. 4 Heat capacity graph at the temperature 0–21 K

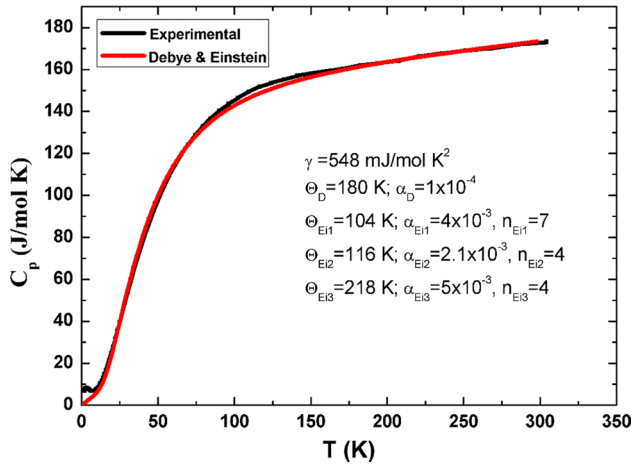

Fig. 6 Fitting of Debye and Einstein formula

Table 2 Comparative study of γ value among different compounds

Compound name	Value of γ (mJ/mol K^2)	References
Ce_4RuMg	137	Current work
Ce_4RuAl	158	[22]
$CeCu_4Al$	92	[23]
$Ce_{23}Ru_7Mg_4$	127	[24]
Ce_2RuZn_4	30	[25]

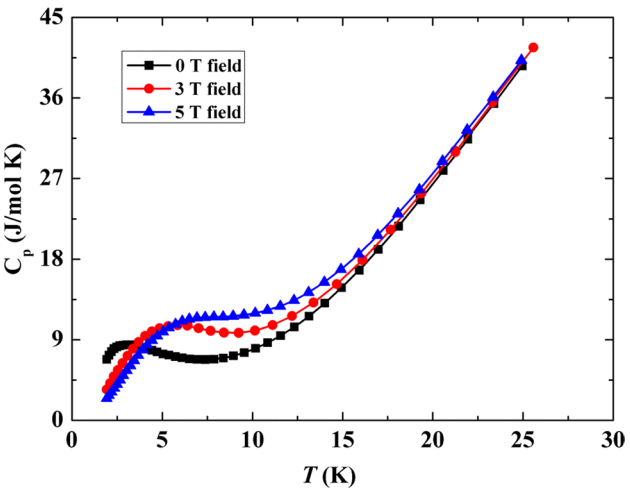

Fig. 5 Heat capacity graph for 0, 3 and 5 T fields

$$C_p(T) = \gamma T + 9NR\left\{\left(\frac{T}{\Theta_D}\right)^3 \int_0^{\Theta_D/T} \frac{x^4 e^x dx}{(e^x-1)^2}\right\} \quad (2)$$

In this equation, N represents the grand sum of atoms in the formula unit. The letters $x = h\omega/k_BT$ and R relate with the gas constant [22–25].

For the complete explanation of specific heat data, we would like to consider the optical modes because it plays a substantial role at higher temperatures. The phonon part can be described by studying the splitting of the phonon spectrum into the acoustic and optical branches. According to Einstein's formula, the following equation expresses the optical modes:

$$C_{Ei}(T) = R\left\{\sum_{i=1}^{6}\left(\frac{\Theta_{Ei}}{T}\right)^2 \frac{e^{\Theta_{Ei}/T}}{(e^{\Theta_{Ei}/T}-1)^2}\right\} \quad (3)$$

In Eq. (3), the symbol Θ_{Ei} expresses the Einstein temperature for all optical branches. The compound's isobaric specific heat has been fitted by using both Einstein and Debye models including their anharmonic correction coefficients α_D and α_{Ei} to determine the variation between the isochoric specific heat and the isobaric specific heat [26, 27]:

$$C_p(T) = \gamma T + R\left\{\frac{9}{1-\alpha_D T}\left(\frac{T}{\Theta_D}\right)^3 \int_0^{\Theta_D/T} \frac{x^4 e^x dx}{(e^x-1)^2}\right\} + R\left\{\sum_{i=1}^{6}\frac{1}{1-\alpha_{Ei}T}\left(\frac{\Theta_{Ei}}{T}\right)^2 \frac{e^{\Theta_{Ei}/T}}{(e^{\Theta_{Ei}/T}-1)^2}\right\} \quad (4)$$

The following parameters have been calculated for the fitting: $\gamma = 548$ mJ/mol K^2 and $\Theta_D = 180$ K and $\Theta_{Ei} = 104$ K, 116 K, 218 K, $\alpha_D = 1.0 \times 10^{-4}$ and $\alpha_{Ei} = 4 \times 10^{-3}$, 2.1×10^{-3}, 5×10^{-3}, respectively. Figure 6 represents the contributions of C_{el} and C_{ph} along with the experimental value of heat capacity of the compound Ce_4RuMg. The value of C_{mag} is calculated by subtracting

the value of the measured specific heat and the value of C_{el+ph}. The contribution of C_{mag} to the specific heat has a direct relation with the energy levels of magnetic ions.

4 Conclusion

The magnetic properties of Ce_4RuMg have been studied from a very low temperature to above room temperature. To have the observation of magnetic properties at very low temperatures, a very low temperature of up to 0.4 K has been considered. A discrete irregularity at 1.5 K represents the antiferromagnetic phase transition and is almost consistent with the measured heat capacity measurements. The observed magnetic properties (susceptibility, phase transition, and heat capacity) suggest the existence of strong electronic correlations in Ce_4RuMg. The enhanced value of $\gamma = 137$ mJ/Ce-mol·K^2 indicates the short-range correlations immediately above T_N.

Acknowledgements J. C. Debnath acknowledges support from the Asian University for Women, Bangladesh in carrying out this research.

Author contributions The corresponding author JCD prepared the samples and did all the experimental tasks and also prepared the draft manuscript. SFA analyzed part of the experimental data and is an expert. JLW made important suggestions throughout the manuscript.

Data availability Not applicable.

Declarations

Ethical statement The manuscript entitled "Electronic correlation Effects in Ce_4RuMg compound" is unique and is not submitted elsewhere for publication.

References

1. P.S. Riseborough, Phys. Rev. B **45**, 13984 (1992)
2. K. Takegahara, H. Harima, Y. Kaneta, A. Yanase, J. Phys. Soc. Jpn. **62**, 2103 (1993)
3. A. Georges, G. Kotliar, W. Krauth, M.J. Rozenberg, Rev. Mod. Phys. **68**, 13 (1996)
4. P.S. Riseborough, Adv. Phys. **49**, 257 (2000)
5. M.B. Maple, R.E. Baumbach, N.P. Butch, J.J. Hamlin, M. Janoschek, J. Low Temp. Phys. **161**, 4 (2010)
6. C.M. Varma, Rev. Mod. Phys. **48**, 219 (1976)
7. G.R. Stewart, Rev. Mod. Phys. **73**, 797 (2001)
8. A. Amato, Rev. Mod. Phys. **69**, 1119 (1997)
9. L.F. Matheiss, D.R. Hamman, Phys. Rev. B **47**, 13114 (1993)
10. J.C. Debnath, S.F. Ahmed, J.L. Wang, Appl. Phys. A **128**, 922 (2022)
11. P. Coleman, in "Handbook of Magnetism and Advanced Magnetic Materials," ed. By H. Knoemuller and S. Parkin, John Wiley and Sons, **1,** 95 (2007).
12. H.V. Lohneysen, A. Rosch, M. Vojta, P. Woelfle, Rev. Mod. Phys. **79**, 1015 (2007)
13. A. Szytu1a, J. Leciejewicz, Handbook of crystal structures and magnetic properties of rare earth intermetallics. Boca Raton: CRC Press; 1994.
14. P. Gegenwart, Q. Si, F. Steglich, Nat Phys **4**, 186 (2008)
15. GR. Stewart, Rev. Mod. Phys. **78**, 743 (2006).
16. R. Settai, T. Takeuchi, Y. Onuki, J. Phys. Soc. Jpn. **76**, 051003 (2007)
17. O. Stockert, S. Kirchner, F. Steglich, Q. Si, J. Phys. Soc. Jpn. **81**, 011001 (2012)
18. H. von Löhneysen, A. Rosch, M. Vojta, P. Wölfle, Rev. Mod. Phys. **79**, 1015 (2007)
19. F. Tappe, C. Schwickert, S. Linsinger, R. Pöttgen, Monatsh. Chem. **142**, 1087 (2011)
20. S.F. Matar, B. Chevalier, R. Pöttgen, Intermetallics **31**, 88 (2012)
21. S. Tuncel, B. Chevalier, S.F. Matar, R. Pöttgen, Z. Anorg. Allg. Chem. **633**, 2019 (2007)
22. J. C. Debnath, Strydom, A. M., Tappe, F., Pottgen, R. "Magnetic and thermodynamic properties of Ce4RuAl". Acta Physica Polonica A, **127,** 237 (2015).
23. M. Falkowski, A. Kowalczyk, T. Tolinski, J. Alloys Compd. **509**, 6135 (2011)
24. J. C. Debnath, Strydom, A. M., Tappe, F., Pottgen, R., (2015). "Magnetic and thermodynamic properties of Ce23Ru7Mg4 compound". SAIP Conf. Proc. **978,** 19 (2015).
25. V. Eyert, E.-W. Scheidt, W. Scherer, W. Hermes, R. Pöttgen, Phys. Rev. B **78**, 214420 (2008)
26. C.A. Martin, J. Phys.: Condens. Matter **3**, 5967 (1991)
27. P. Svoboda, P. Javorsk´y, M. Divis, V. Sechovsk´y, F. Honda, G. Oomi, A. A. Menovsky, Phys. Rev. B **63,** 212408 (2001).